Trace analysis of nitrated polycyclic aromatic hydrocarbons based on two-color femtosecond laser ionization mass spectrometry

Wen, Lu
Faculty of Design, Kyushu University

Yoshinaga, Katsunori
Faculty of Design, Kyushu University

Imasaka, Totaro
Kyushu University

Imasaka, Tomoko
Faculty of Design, Kyushu University

出版情報：Talanta. 265, pp.124807-, 2023-12-01. Elsevier
バージョン：
権利関係：

Trace analysis of nitrated polycyclic aromatic hydrocarbons based on two-color femtosecond laser ionization mass spectrometry

Lu Wen [a], Katsunori Yoshinaga [a], Totaro Imasaka [b,c], Tomoko Imasaka [a,*]

[a] *Faculty of Design, Kyushu University, 4-9-1, Shiobaru, Minami-ku, Fukuoka 815-8540: 744 Motooka, Nishi-ku, Fukuoka 819-0395, Japan*

[b] *Kyushu University, 744 Motooka, Nishi-ku, Fukuoka 819-0395, Japan*

[c] *Hikari Giken, Co., 2-10-30, Sakurazaka, Chuou-ku, Fukuoka 810-0024, Japan*

* Corresponding author.

Graduate School of Design, Kyushu University, 4-9-1, Shiobaru, Minami-ku, Fukuoka 815-8540, Japan

E-mail address: imasaka@design.kyushu-u.ac.jp (Tomoko IMASAKA)

ABSTRACT

Nitrated polycyclic aromatic hydrocarbons (nitro-PAHs) are suspected to be highly carcinogenic and mutagenic compounds that are present in the environment. Gas chromatography combined with mass spectrometry (GC-MS) is the most frequently used technique for trace analysis. The electron ionization techniques that are currently used in MS, however, typically do not result in the formation of a molecular ion, thus making the determination of these compounds more difficult. In this study, we report on the use of a compact highly-repetitive (low-pulse-energy) ultraviolet (UV) femtosecond laser as the ionization source in combination with a miniature time-of-flight mass analyzer and a time-correlated ion counting system. The UV laser pulses emitted at 343, 257, and 206 nm were produced by harmonic generations of a femtosecond Yb laser emitting at 1030 nm and were utilized for single-color multiphoton ionization. A combination of the 343-nm and 257-nm pulses was further employed to achieve two-color two-photon ionization. This technique was found to be more useful for sensitive detection and also resulted in the formation of a molecular ion. A pump-and-probe technique using these pulses was examined in a proof-of-concept study to measure the femtosecond lifetimes of the nitro-PAHs separated by GC, providing additional information for use in the characterization of the analyte. The developed technique was applied in the analysis of an authentic sample, an organic solvent extract from diesel exhaust particulates. The nitro-PAHs contained in a standard reference material (SRM1975) were determined on a two-dimensional GC-MS display, suggesting that this technique would be useful for the practical trace analysis of nitro-PAHs in environmental samples.

Keywords:

Multiphoton ionization; mass spectrometry; two-color femtosecond laser; nitrated polycyclic aromatic hydrocarbon; standard reference material

1. Introduction

Nitrated polycyclic aromatic hydrocarbons (nitro-PAHs) are analogs of polycyclic aromatic hydrocarbons (PAHs) that contain at least one nitro group in the molecule. They are directly produced by combustion of fossil fuels and also by chemical reactions of PAHs with O_3 and NO_2 in the atmosphere [1-3]. Different types of nitro-PAHs are formed as the result of the atmospheric transformation of PAHs. In fact, 30-40% of the mutagenicity was contributed by 1,3-, 1,6-, and 1,8-dinitropyrene, 1-nitropyrene and 3- and 8-nitrofluorancene in a sample extracted form diesel exhaust particulates [2]. When nitro-PAHs are inhaled into the human body, this exposure increases oxidative stress thus increasing the risk of developing cardiovascular disease [3]. As a result, nitro-PAHs are used as special source markers [3, 4]. However, transformations of these compounds that occur in the environment are still a subject of debate, since photochemical decomposition is considered to be a major factor in decreasing the concentration of nitro-PAHs. Although the levels of these compounds are much lower than those of PAHs, nitro-PAHs have a more potent carcinogenicity and mutagenicity [3, 4]. Indeed, the concentrations of nitro-PAHs that are typically adsorbed on particulate matter are 10-100 times lower than

those of PAHs [5, 6]. However, the mutagenicity and carcinogenicity of these nitro-PAHs are reported to be 200-110000 times higher than that for benzo(a)pyrene [7]. Therefore, a sensitive as well as a selective method for the analysis of nitro-PAHs is clearly needed.

A variety of analytical techniques have been developed for measuring nitro-PAHs in the environment [8]. Liquid chromatography combined with electrochemical detection, fluorescence detection, or chemiluminescence detection, has been employed, although a chemical reaction is needed in these techniques [9-12]. Among them, the most sensitive technique is reported to be chemiluminescence with detection limits of 0.1-10 pg (cf. fluorescence 1-10 pg) [12]. Many techniques involve the use of gas chromatography combined with various detectors, e.g., flame ionization detector, nitrogen-phosphorus detector, and electron capture detector [13-16]. The most frequently used technique is gas chromatography coupled with mass spectrometry (GC-MS), because of the superior separation resolution given by GC and the excellent sensitivity provided by MS. It should be emphasized that MS is very useful for the identification of analyte molecules. Many types of MS with different ionization sources have been developed to date. Among them, electron ionization (EI) is widely used in conventional MS [17-20]. In order to improve the sensitivity of this method, it is necessary to improve the selectivity for background suppression. High-resolution MS operated in the selected-ion monitoring (SIM) mode (HR(SIM)MS) has been utilized for this purpose [21]. However, some organic compounds (including nitro-PAHs) dissociate readily, and fragment ions are dominantly observed in EIMS. This can make it difficult to determine the molecular weight of the analyte by observing a molecular ion and to identify the analytes contained in a complex sample matrix. To solve this problem, positive/negative ion chemical ionization MS (PICI/NICIMS) has been developed, since it provides a molecular ion [22-26]. This

approach is particularly useful for measuring highly electronegative compounds such as nitro-PAHs, since it provides excellent selectivity and sensitivity. However, identifying the analyte by finger-printing is difficult due to a lack of a fragment pattern. Another approach to improving selectivity is the use of a hyphenated technique such as MS/MS and GC×GC. Mass analyzed ion kinetic energy spectrometry (MIKES)-MS/MS and triple-stage quadrupole (TSQ)MS/MS have been developed for this purpose [17]. These techniques were employed in a study of the decay/formation mechanism of PAHs/nitro-PAHs in the environment [18]. A two-dimensional separation technique coupled with MS such as GC×GC-MS/MS has superior selectivity and is now frequently used in trace analysis [21]. However, these techniques make the comprehensive analysis of unknown nitro-PAHs difficult.

A photoionization technique has been developed to improve both the selectivity and the sensitivity of this technique [27]. The ionization energy (*IE*) of nitro-PAHs is 7-11 eV, and 1-nitronaththalene was measured by single-photon ionization in MS using a vacuum-ultraviolet (VUV) nanosecond laser [28]. On the other hand, the excitation energy (*EE*) of nitro-PAHs is 3-4 eV, and such a molecule can be efficiently ionized by absorbing the first photon for excitation and the subsequent photon for ionization, a process referred to as resonance-enhanced two-photon ionization (RE2PI), or more generally as resonance-enhanced multiphoton ionization (REMPI). For example, a solid sample was directly vaporized and ionized using ultraviolet (UV) nanosecond lasers (266 and 213 nm, 8 ns) for observing positive and negative ions, which provided limits of detection (LODs) at the picomole level [29- 30]. A near-infrared (NIR) femtosecond laser (800 nm, 10 mJ, 10 Hz) was used for MPI after laser desorption of a sample using a UV nanosecond laser (266 nm) [31]. To measure a sample in a complex matrix, GC was

combined with MS using UV and NIR femtosecond laser ionization sources (fsLIMS) [32]. Indeed, this technique has been applied to the trace analysis of nitro-PAHs in a complex matrix at the sub-picogram level [33-36]. Note that nitro-PAHs were converted into amino-PAHs for more sensitive/selective detection before mass analysis [37, 38]. Nitro-PAHs have very short lifetimes and relax to the ground state on the femtosecond time scale. Therefore, it is desirable to use a femtosecond laser for efficient RE2PI. In this technique, a molecular ion as well as large fragment ions is enhanced significantly, which was then useful for the assignment of the analyte. It was, however, necessary to use an MS comprised of a large mass analyzer and a complicated laser system consisting of a Ti:sapphire laser, an optical parametric amplifier, and harmonic generators as the ionization source, which prevented the practical analytical use of this approach. In order to improve ionization efficiency, it was suggested that the analyte be ionized when measurements are made at around 200 nm because of a strong absorption band located at shorter wavelengths. This, however, resulted in significantly increased background signals that arose from interferences present in a complex sample mixture. To suppress these undesirable signals, it was suggested that the nitro-PAHs be measured in the near-UV region (345 nm) in the case of an actual trace analysis [34]. In addition, it is preferable to decrease the excess energy remaining in the ionic state so as to suppress fragmentation. As a result, it would be preferential to use two femtosecond pulses emitting at different wavelengths, since the first pulse can be used for optimal excitation and the second pulse for optimal ionization. This would minimize the effect of interferences and suppress fragmentation.

In this study, we report on the analysis of a standard sample mixture containing 14 nitro-PAHs (see Fig. 1 for their chemical structures) based on GC-MS using the harmonic

emissions of a compact femtosecond Yb laser as the ionization source. The UV pulses emitting at 343, 257, and 206 nm were generated and used for single-color and two-color ionizations to analyze the standard sample mixture and also a real sample extracted from diesel exhaust particulates. Furthermore, the two-color pump-and-probe technique was examined in a proof-of-concept study to obtain additional information concerning the lifetime of the analyte molecule and to improve selectivity in spectrometric analysis.

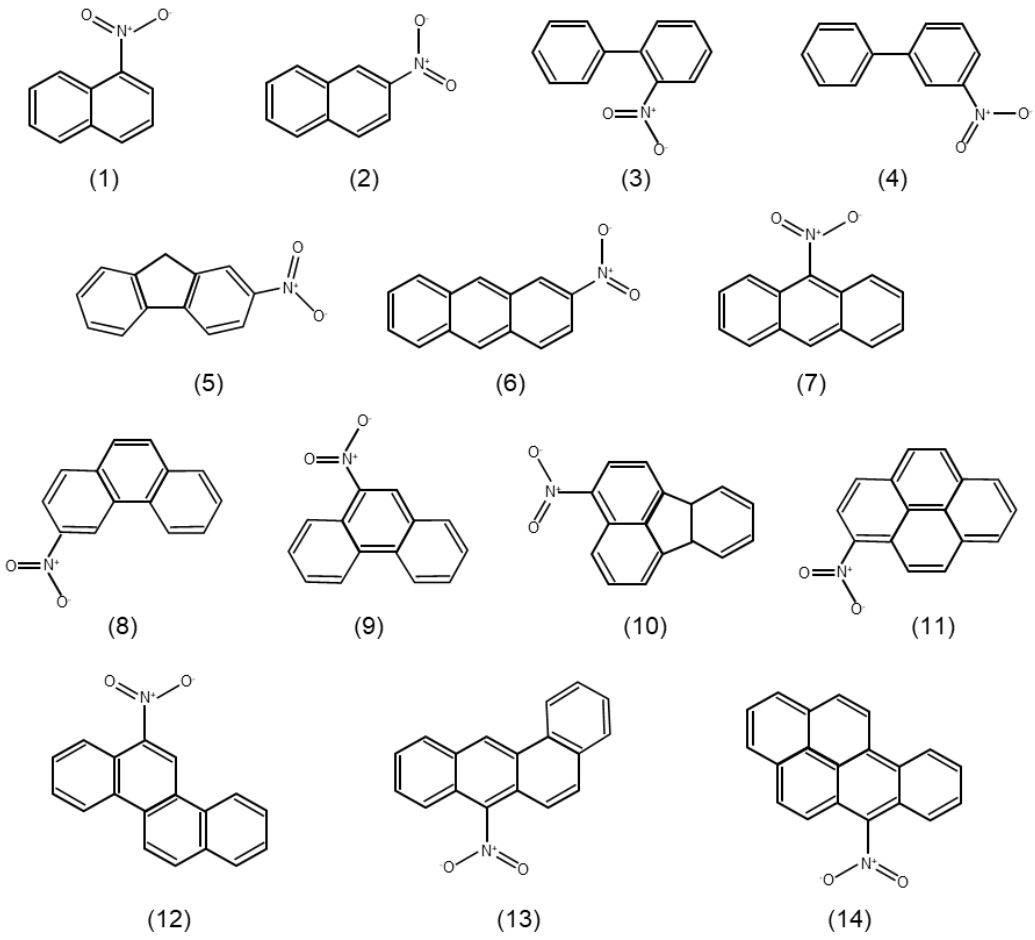

Fig. 1. Chemical structures of the nitro-PAHs examined in this study. (1) 1-nitronaphthalene [173] (2) 2-nitronaphthalene [173] (3) 2-nitrobiphenyl [199] (4) 3-nitrobiphenyl [199] (5) 2-nitrofluorene [211] (6) 2-nitroanthracene [223] (7) 9-nitroanthracene [223] (8) 3-nitrophenanthrene [223] (9) 9-nitrophenanthrene [223] (10) 3-nitrofluoranthene [247] (11) 1-nitropyrene [247] (12) 6-nitrochrysene [273] (13) 7-nitrobenz(a)anthracene [273] (14) 6-nitrobenzo(a)pyrene [297]. [ ]: molecular weight.

2. Material and methods

2.1. Analytical instrument

A block diagram of the experimental apparatus used in this study is shown in Fig. S1 in the Supplementary Material. Briefly, the sample was measured by a GC (6890 N, Agilent Technologies) combined with a miniature time-of-flight (TOF) mass analyzer (flight tube length 65 mm, mass resolution 670) that was recently developed in our laboratory [39]. The analyte eluting from GC was introduced into the mass analyzer maintained at ~ 4×10^{-3} Pa using a fused silica capillary. A femtosecond Yb laser (wavelength 1030 nm, pulse width 400 fs, output power 2.4 W, pulse repetition rate 120 kHz, Calmer Laser) was employed as a fundamental beam to generate the third (343 nm), fourth (257 nm), and fifth (206 nm) harmonic emissions. The two beams, e.g., the third and fourth harmonic emissions, were separated and recombined using dichroic mirrors. A mechanical stage with the dielectric mirrors mounted on it was translated using a high-precision micrometer head (resolution 1 μm) to adjust the time delay between the two pulses. The combined beam was confocally focused together using a pair of UV-enhanced concave and flat aluminum mirrors onto an analyte in a molecular beam in the MS, in order to avoid mismatching of the focal lengths at different wavelengths when using a fused silica lens. The angle between the molecular beam and the laser beam was slightly tilted (ca. 10 degree) to increase the interaction volume and to improve the ionization efficiency [39]. The ions produced by MPI were accelerated toward a TOF tube (no delay extraction field available) and were detected by an assembly of microchannel plates (response time ca. 600 ps, F14844eY002, Hamamatsu Photonics). The signal was amplified by 60-fold using an amplifier (bandwidth 1.5 GHz, C5594, Hamamatsu

Photonics), and the output signal was measured by a time-to-digital converter (time resolution 250 ps, TimeHarp 260 NANO, PicoQuant) installed in a personal computer.

A 1-μL aliquot of sample solution was injected into the GC by means of an auto sample injector (splitless mode), and the analytes were separated on a capillary column (DB-5MS, length 30 m, inner diameter 0.25 mm, film thickness 0.25 mm, Agilent Technologies). Helium was used as a carrier gas, and the flow rate was adjusted to 1 mL/min. The temperature of the sample injection port was set at 280 ℃, which was a compromise that allowed all 14 nitro-PAHs studied here to be measured (dependence of the signal intensity on the temperature of the sample injection port is shown in Fig. S2). The temperature program of the capillary column was as follows: the oven temperature was increased from 40 ℃ (held for 1 min) to 120 ℃ at a rate of 20 ℃/min (held for 1 min), then increased to 280 ℃ at a rate of 5 ℃/min (held for 10 min). The temperature of the transfer line between the GC and the MS was maintained at 300 ℃.

2.2. Reagents and chemicals

CAUTION: Nitro-PAHs are potent direct-acting mutagens and carcinogens, and precautions should be taken to prevent dermal and inhalation exposure to nitro-PAH solutions and vapors. A standard sample mixture containing 2-nitronaphthalene, 2-nitroanthracene, 9-nitroanthracene, 3-nitrophenanthrene, 9-nitrophenanthrene, 6-nitrochrysene, 7-nitrobenz(a)anthracene, and 6-nitrobenzo(a)pyrene was purchased from AccuStandard. Six nitro-PAHs, i.e., 1-nitronaphthalene, 2-nitrobiphenyl, 3-nitrobiphenyl, 2-nitrofluorene, 3-nitrofluoranthene, and 1-nitropyrene were purchased from Sigma-

Aldrich Japan, which were dissolved in toluene (Wako Pure Chemical Industries, Ltd.) and were diluted with acetonitrile manufactured for chromatography (Wako Pure Chemical Industries, Ltd.). A standard sample mixture containing the 14 nitro-PAHs was prepared by mixing these standard solutions. The concentration was adjusted to 6.5 ppm for each by diluting with acetonitrile. This stock solution was diluted stepwise with acetonitrile and was used in the experiments. Standard Reference Material 1975 (SRM1975) supplied from National Institute of Standard and Technology (NIST), which was extracted from diesel exhaust particulates, was used as an example of a real sample for performance evaluation of the analytical instrument.

3. Results and discussion

3.1. Spectral properties

The absorption spectra were calculated for the 14 nitro-PAHs. The results are shown in Fig. S3 (see the absorption spectra calculated by density functional theory, DFT), and the spectral properties are summarized in Table S1. In single-color ionization, nitro-PAHs are ionized mainly through RE2PI at 257 and 206 nm and through resonance-enhanced three-photon ionization (RE3PI) or nonresonant three-photon ionization (NR3PI) at 343 nm depending on the molecule. In two-color ionization that is achieved using a combination of optical pulses at 257 and 343 nm, nitro-PAHs can be ionized through RE2PI or nonresonant two-photon ionization (NR2PI) for large molecules, which is in contrast to RE3PI or nonresonant three-photon ionization (NR3PI) for small molecules, depending on the order of introducing the two optical pulses, e.g., 257 nm (first) + 343 nm (second), referred to as “257 + 343 nm”, and vice versa. It is noteworthy that the

excess energy can be reduced by using a two-color RE2PI scheme (total photon energy 8.43 eV) for large nitro-PAHs and by single-color RE3PI/NR3PI (total photon energy 10.83 eV) for small nitro-PAHs (see the caption of Table S1).

3.2. Two-dimensional display of GC-MS for a standard sample mixture

Figure 2 shows a two-dimensional GC-MS display that was measured for a standard sample mixture containing 14 nitro-PAHs, based on two-color ionization using the optical pulses at 257 + 343 nm (three two-dimensional displays of GC-MS measured at 343, 257, and 206 nm are shown in Fig. S4). The analytes were separated in the order of volatility

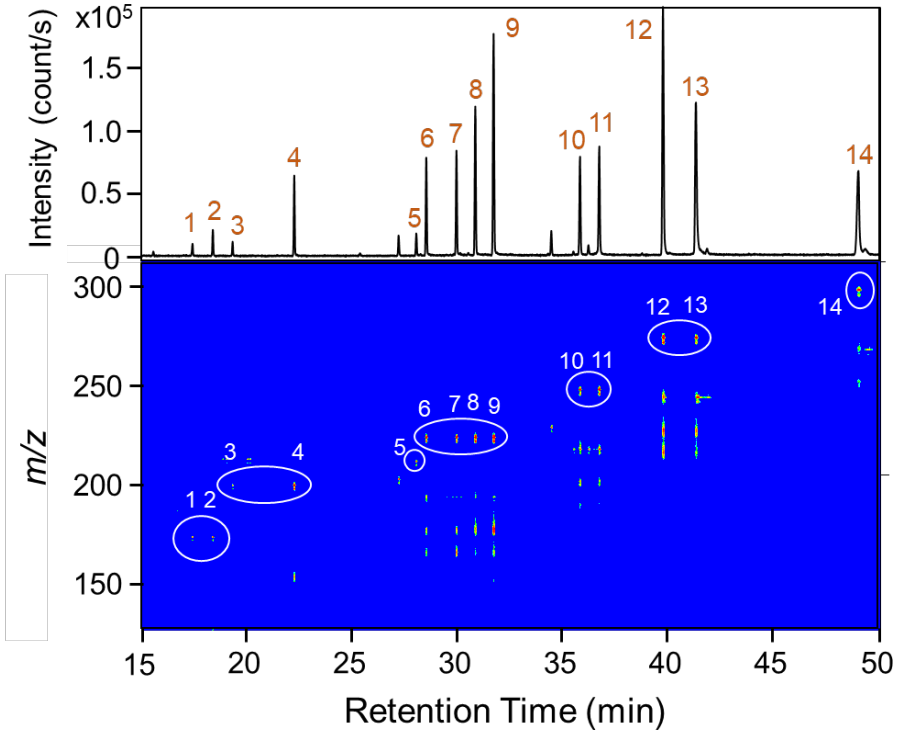

Fig. 2. Two-dimensional display of GC-MS measured for a sample mixture containing 14 nitro-PAHs (6.5 ppm for each) ionized using a combination of UV pulses at 343 (70 mW) and 257 nm (90 mW). The delay time was adjusted to $t_{DL} = 0$. A total ion chromatogram is shown at the top of the figure. The signals with numbers can be assigned to 14 nitro-PAHs (see the chemical structures shown in Fig. 1), and the other signals with no number are attributed to impurities in the sample. The signals arising from the molecular ions are indicated by circles in the figure.

that is mainly determined by the molecular weight of the analyte, since a slightly polar capillary column (DB-5MS) was used for GC separation. The mass spectra measured at the retention times, at which four compounds appear, were extracted from Figs. 2 and S4 and are shown in Fig. 3. A large signal arising from a molecular ion was observed in mass spectra for all of the nitro-PAHs. The situation remained unchanged even when three photons were required for ionization at 343 nm. This favorable result can be attributed to rather efficient RE3PI for large nitro-PAHs such as 6-nitrochrysene (see Table S1), which can be preferentially used for selective determination of nitro-PAHs. Note that even small nitro-PAHs such as 3-nitrobiphenyl can be ionized with sufficient efficiency via NR3PI because of a short optical pulse width (high peak power) and the large output power of

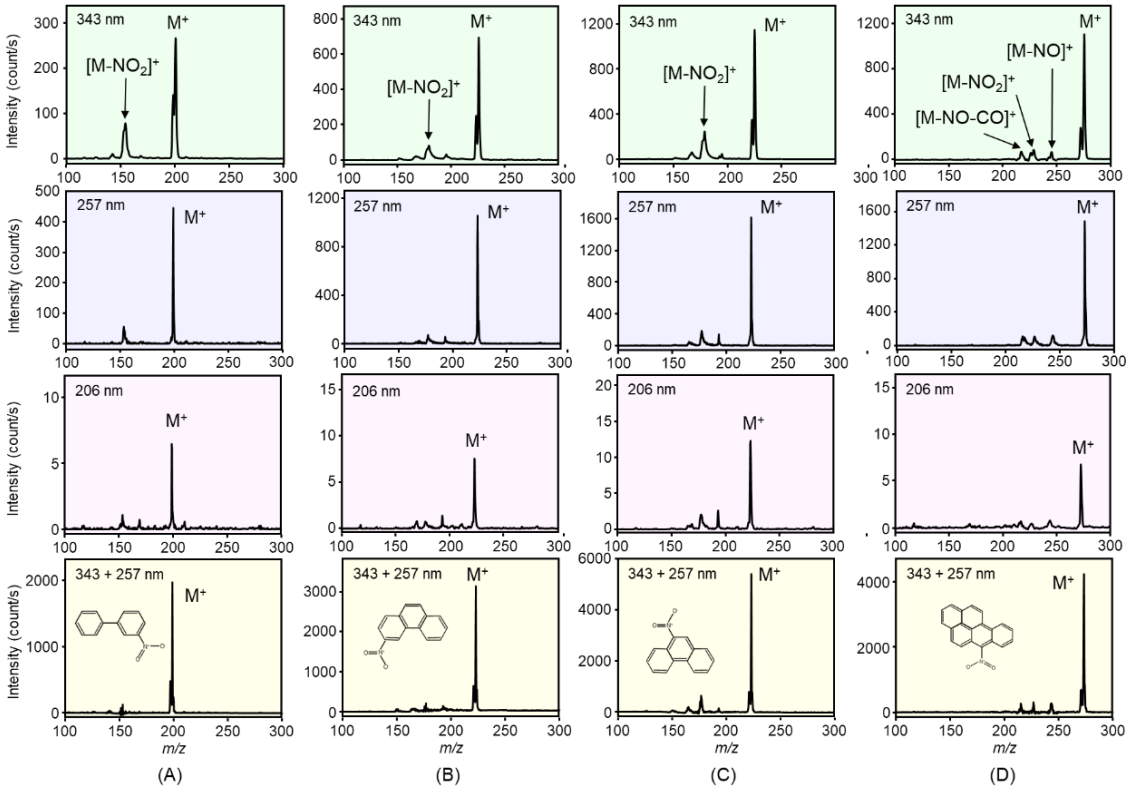

Fig. 3. Mass spectra measured at 343 nm (140 mW), 257 nm (140 mW), 206 nm (29 mW), and 343 nm (70 mW) + 257 nm (90 mW) at t_{DL} = 0. (A) 3-nitrobiphenyl (B) 3-nitrophenanthrene (C) 9-nitrophenanthrene (D) 6-nitrochrysene. The data were extracted from the two-dimensional data shown in Figs. 2 and S4. Since the analytes were measured at the same concentration (6.5 ppm for each), the signal intensity (the y-axis) is in proportion to the ionization efficiency at different wavelengths.

the third harmonic emission (140 mW). It is interesting to note that a fragment ion of [M-1]$^+$ was always observed only when the third harmonic emission (343 nm) was used for ionization, suggesting a unique ionization channel associated with the dissociation of a hydrogen atom at the three-photon energy of 10.83 eV. A molecular ion, [M]$^+$, as well as large fragment ions such as [M−NO]$^+$, [M−NO_2]$^+$, and [M−NO−CO]$^+$, was enhanced at 257 nm, since all of the nitro-PAHs were efficiently ionized through RE2PI and a smaller excess energy (two-photon energy 9.63 eV), in addition to a large output power of the fourth harmonic emission (140 mW). On the other hand, the signal intensity was rather low at 206 nm, because of a large excess energy (two photon energy 12.04 eV) and a low output power of the fifth harmonic emission (29 mW). When a two-color ionization scheme was used, larger signals were observed for molecular ions because of efficient RE2PI, a small excess energy (two photon energy 8.43 eV), and a large total output power at 343 nm (70 mW) and 257 nm (90 mW). It should be noted here that the signal intensity of the fragment ion, [M−NO]$^+$, was sometimes very weak, e.g., 3-nitrobiphenyl, as shown in Fig. 3 (A), although the fragment ion of [M−NO_2]$^+$ as well as [M−NO−CO]$^+$ was more clearly observed for all of the nitro-PAHs. This is probably due to the fact that a nitro-nitrite rearrangement is necessary for a C–ONO to be formed prior to the dissociation of NO. On the other hand, there are two possibilities for producing [M−NO_2]$^+$, i.e., one being the direct cleavage of the C–NO_2 bond of a molecular ion and the other being the cleavage of the C-ONO bond after the rearrangement [29, 31, 40]. The fragment ion undergoes further dissociation by breaking the ring structure, which results in the production of a variety of $C_xH_y^+$ fragment ions [31]. It is interesting to note that the fragmentation can be controlled by using a chirp optical pulse of the femtosecond laser [41].

3.3. Comparison

In MPI, the excess energy in the ionic state can be reduced by optimizing the laser wavelengths and the molecular ion can be enhanced, which is beneficial for the identification of nitro-PAHs. Table 1 shows the ratio of the signal intensities, $[M]^+/[F]^+$,

Table 1

Comparison of the $[M]^+/[F]^+$ values measured using fsLIMS and EIMS.

	Compound	This work	EIMS (NIST)	fsLIMS (reported)
1	1-nitronaphthalene (173/127)	22	0.63	NA
2	2-nitronaphthalene (173/127)	5.5	0.92	NA
3	2-nitrobiphenyl (199/143)	46.8	0.38 (/152)	NA
4	3-nitrobiphenyl (199/153)	8.5	0.9 (/152)	NA
5	2-nitrofluorene (211/165)	12.7	0.6	NA
6	2-nitroanthracene (223/177)	11.2	NA	NA
7	9-nitroanthracene (223/165)	9.5	1.63 (/176)	1.6[1)], 0.68[2)], 0.8[3)], 8.9[4)]
8	3-nitrophenanthrene (223/177)	19.0	NA	NA
9	9-nitrophenanthrene (223/177)	7.8	0.61 (/165)	NA
10	3-nitrofluoranthene (247/217)	6.7	1.38 (/200)	1.0[1)], 0.56[2)], 1.2[3)], 2.5[4)]
11	1-nitropyrene (247/217)	5.4	0.84 (/201)	1.2[1)], 0.56[2)], 1.2[3)], 5.0[4)]
12	6-nitrochrysene (273/243)	15.7	1.32 (/226)	NA
13	7-nitrobenz(a)anthracene (273/227)	7.4	NA	NA
14	6-nitrobenzo(a)pyrene (297/267)	10.9	1.21 (/251)	NA

The *m/z* values of the molecular ion and the largest fragment ion are shown in parenthesis. NA, not available. The values reported in this work were obtained using a two-color ionization scheme (257 + 343 nm) at t_{DT} = 0. The $[M]^+/[F]^+$ values were measured at 345 nm[1)] [34] and 400 nm[2)], 800 nm[3)], and 1200 nm[4)] [36]. Large values were obtained at 1200 nm due to no absorption band for ionic species of nitro-PAHs (see the details in the reference: [36]).

in which $[M]^+$ is the molecular ion and $[F]^+$ is the largest fragment ion in MS. As expected, the molecular ion was strongly enhanced in this study. The intensity of the fragmentation ion can, if necessary, be increased by tightly focusing the laser beam onto the molecular beam, permitting finger-printing identification of the analyte. On the other hand, the signal intensity of the molecular ion is rather small in EIMS, making the identification of an analyte more difficult due to congested signals observed in the case of measuring a real sample. Table 2 shows the observed LODs compared with the reported data [20, 33, 34]. The values were in the 0.03-0.38 pg range for the 14 nitro-PAHs used in this study. Higher values for small nitro-PAHs can be attributed to RE3PI/NR3PI, which is less efficient than RE2PI/NR2PI for large nitro-PAHs. These values are smaller than the reported values of 4.5-22.2 pg obtained by GC-EIMS and 20-28 pg obtained by GC-EI/HR(SIM)MS [21]. The LODs can be improved by two orders of magnitude by using present GC-fsLIMS. This favorable result was obtained by optimal two-color MPI, which is useful for the more sensitive detection of nitro-PAHs and for the suppression of the background signal arising from interferences. It should be noted that the LODs achieved here are several times lower than the values reported using a large (more expensive) fsLIMS consisting of a complicated Ti:sapphire laser/optical parametric amplifier/harmonic generator system. This favorable result can be attributed to the use of a higher-average-power low-pulse-energy (low-cost) femtosecond Yb laser that increases the signal intensity and reduces the number of subsequent photons to be absorbed from the ionic state, in addition to a combination of the two pulses emitting at optimal wavelengths to minimize the excess energy. The present LODs were comparable to the 0.03-0.07 pg and 0.09-12 pg values obtained by GC-NCI(SIM)MS [22-26] and 0.03-0.11 pg obtained by GC×GC-MS/MS [21]. As mentioned above, these techniques, however,

Table 2

Comparison of the LODs measured using EIMS and fsLIMS.

	Compounds	This work (pg)	EIMS (ref. 20) (pg)	fsLIMS (reported) (pg)
1	1-nitronaphthalene	0.2	22	NA
2	2-nitronaphthalene	0.38	16.4	NA
3	2-nitrobiphenyl	0.27	16.8	NA
4	3-nitrobiphenyl	0.06	19.1	NA
5	2-nitrofluorene	0.31	8.8	NA
6	2-nitroanthracene	0.06	10.9	NA
7	9-nitroanthracene	0.13	4.5	0.2[1)], 0.94[2)], 0.54[3)], 0.42[4)]
8	3-nitrophenanthrene	0.04	22.2	NA
9	9-nitrophenanthrene	0.03	11.5	NA
10	3-nitrofluoranthene	0.08	10.8	0.3[1)], 0.20[2)], 1.09[3)], 1.19[4)]
11	1-nitropyrene	0.07	14.5	0.3[1)], 0.27[2)], 0.68[3)], 0.93[4)]
12	6-nitrochrysene	0.05	8.0	NA
13	7-nitrobenz(a)anthracene	0.06	17.7	NA
14	6-nitrobenzo(a)pyrene	0.13	8.5	NA

The LODs were measured at 345 nm[1)] [33] and at 200 nm[2)], 267 nm[3)], and 343 nm[4)] [34]. NA, not available.

make a comprehensive analysis of unknown nitro-PAHs difficult. Note that the LODs obtained in this study could be further improved by using a cool on-column (or cooled) sample injection method in GC to reduce the thermal decomposition of nitro-PAHs (see Fig. S2) [21, 26].

3.4. Pump-and-probe technique

A pump-and-probe technique is currently used for measuring femtosecond lifetimes of the excited states for large molecules such as pyrene [42]. In this study, this technique was examined in an attempt to study dynamics of nitro-PAHs and to improve the selectivity in the spectrometric analysis, in which the two-color two-photon ionization scheme (343 + 257 nm) was utilized because of the larger signal intensity (see Fig. 3) and lower background signals arising from interference such as PAHs when a real sample was measured at shorter wavelengths (e.g., at 267 nm) [33,34].

3.4.1. Model

Figures 4 (A) and (B) show the energy diagrams for the ionization of nitro-PAHs that were used in this study. The signal intensity of the molecular ion can be calculated by equations (1) and (2) (see the details for derivation of the equations shown in the Supplementary Material).

$$[N_2] = k_{3A} I_{(343)} [N_1]_0 e^{-(t_{DT}/\tau_A)} \quad (1)$$

$$[N_2] = k_{3B} I_{(257)} [N_1]_0 e^{-(t_{DT}/\tau_B)} \quad (2)$$

where $[N_1]_0$ and $[N_2]$ are the populations of the excited state immediately after excitation and of the ionic state, respectively, k_{3A} and k_{3B} are the rate constants for ionization, $I_{(343)}$ and $I_{(257)}$ are the intensities of the optical pulses at 343 nm and 257 nm, respectively, t_{DT} is the delay time between the 257-nm and 343-nm pulses, τ_A and τ_B are the lifetimes of excited states A and B, respectively. The ratio of the signal intensities, $[M]^+/[F]^+$, can be calculated by equations (3) and (4).

$$\frac{[M]^+}{[F]^+} \sim e^{-(t_{DT}/\tau_A)} + K_5 \quad (t_{DT} \leq 0) \tag{3}$$

$$\frac{[M]^+}{[F]^+} \sim e^{-(t_{DT}/\tau_B)} + K_5 \quad (t_{DT} \geq 0) \tag{4}$$

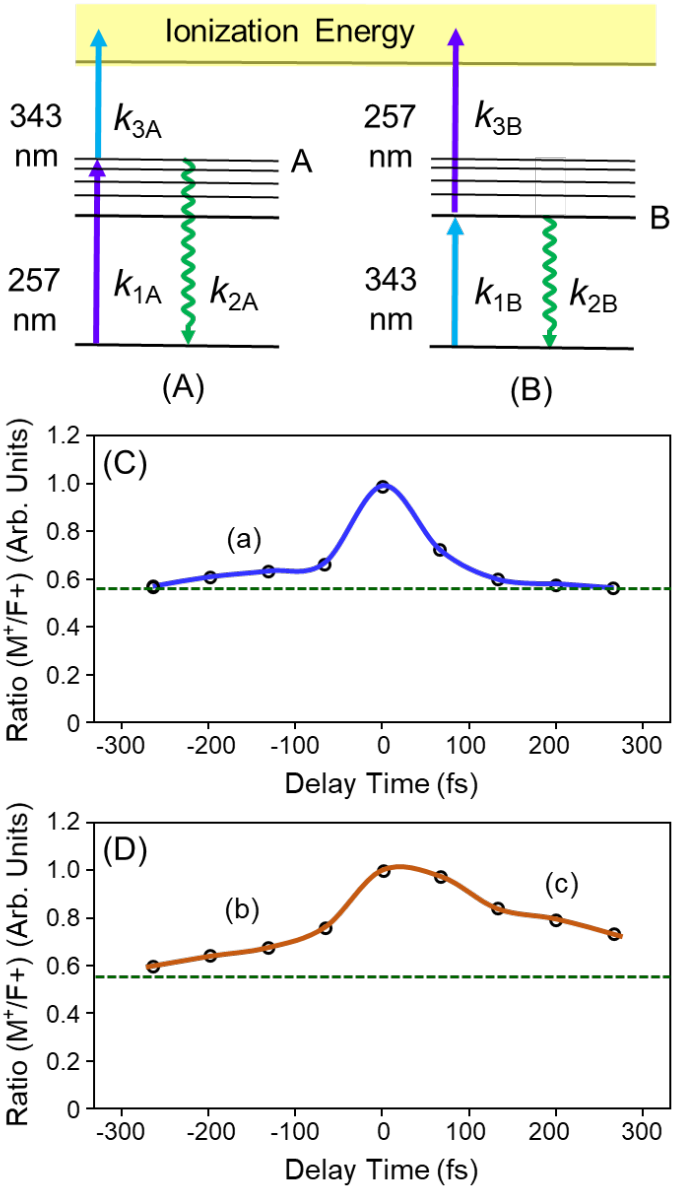

Fig. 4. Energy diagram of two-color two-photon ionization at (A) 257 + 343 nm (B) 343 + 257 nm and dependence of the ratio, $[M]^+/[F]^+$, on the delay time between the excitation (pump) and ionization (probe) pulses for (C) 1-nitronaphthalene (D) 3-nitrofluoranthene. The pump pulse (257 nm) appears earlier than the probe pulse (343 nm) at negative delay times ($t_{DL} < 0$).

where K_5 is a constant and is independent of the delay time. The lifetime of the excited state can then be evaluated by measuring the value of $[M]^+/[F]^+$ at different time delays.

3.4.2. Evaluation of the laser pulse width

The dependence of the signal intensity on the laser power was measured by continuously introducing acetonitrile into the MS (see Experimental Procedures in the Supplementary Material). The slope in the log-log plot was 1.8 (see the observed data shown in Fig. S5), suggesting nonresonant two-photon ionization under present conditions. MS can then be used as a two-photon detector in a cross correlator to evaluate the laser pulse width [43]. A cross correlation trace was measured using the third (343 nm) and fourth (257 nm) harmonic emissions, and the optical pulse width was determined to be 150 fs from the full width at half maximum of the observed data (the relationship between the signal intensity and the delay time is shown in Fig. S6).

3.4.3. Lifetime measurement

Figures 4 (C) and (D) show the dependences of the $[M]^+/[F]^+$ ratio obtained by changing the delay time between the optical pulses at 257 and 343 nm (the pulse at 257 nm appears earlier than the pulse at 343 nm at $t_{DT} < 0$). The maximum value was obtained at $t_{DT} = 0$, since these molecules can reach the *IE* with nearly zero excess energy (see Table S1) and are efficiently ionized before vibrational relaxation. A very short decay of less than 150 fs (or no decay) was observed for 1-nitronaphthalene at $t_{DT} > 0$, due to the NR3PI process. In contrast, a double exponential decay was observed at $t_{DT} < 0$, due to RE3PI as shown in Fig. 4 (C) (a), and the lifetime of the longer decay was calculated to be 360 fs from the slope of the semi-log plot shown in Fig. S7 (the data for the semi-log

plot of the signal intensity vs. the delay time). A decay was more clearly observed for 3-nitrofluoranthene, as shown in Fig. 4 (D) (b) and (c), and the lifetimes were calculated to be 220 and 510 fs from the data shown at $t_{DT} < 0$ and $t_{DT} > 0$, respectively (see the observed data shown in Fig. S7). The longer lifetime observed by exciting at 343 nm can be explained by less efficient vibrational relaxation from the lower excited state with a lower density of vibrational levels. These femtosecond lifetimes are in reasonably good agreement with lifetimes of 70 fs for 1-nitronaphthalene and 50 fs and 1.3 ps (double exponential decay) for 3-nitrofluoranthene in methanol measured by femtosecond fluorescence up-conversion at an exciting wavelength of 385 nm [44]. It should be noted that the lifetime of 1-nitropyrene is reported to be 200-820 fs and 2.9-9.0 ps (double exponential decay), depending on the fluorescence wavelength being used and also on the dielectric constant of the solvent being used, which affects the rate of intersystem crossing [45]. As demonstrated, a pump-and-probe technique provides information concerning the excited-state lifetimes of a molecule and then for characterization of the analyte and additional selectivity in spectrometric analysis. This technique can be applied for a variety of organic compounds such as PAHs, although the probe pulse should be delayed more than 3 m for a PAH molecule with a lifetime of 10 ns (0.3 m/ns × 10 ns = 3 m). In this study, the decay curve was prepared by injecting the sample into the GC ca. 10 times at different delay times, due to strong carcinogenicity and mutagenicity of nitro-PAHs (see the precaution in the *Reagents and chemicals*), preventing accurate measurements of the decay curve. It would be possible to more accurately measure a decay curve "on the fly" for isolated (gaseous) nitro-PAHs eluting from the GC, since a mass spectrum can be measured every 0.1 s in the present analytical system and the time delay can readily be scanned repetitively using a computer-controlled delay stage.

3.5. Application to a real sample

Figure 5 shows the two-dimensional display of GC-MS obtained by using a two-color ionization scheme for a real sample (SRM1975). Numerous signals arising from PAHs and nitro-PAHs were observed (the concentrations of nitro-PAHs calculated from the observed data and the non-certified values reported by NIST are summarized in Table

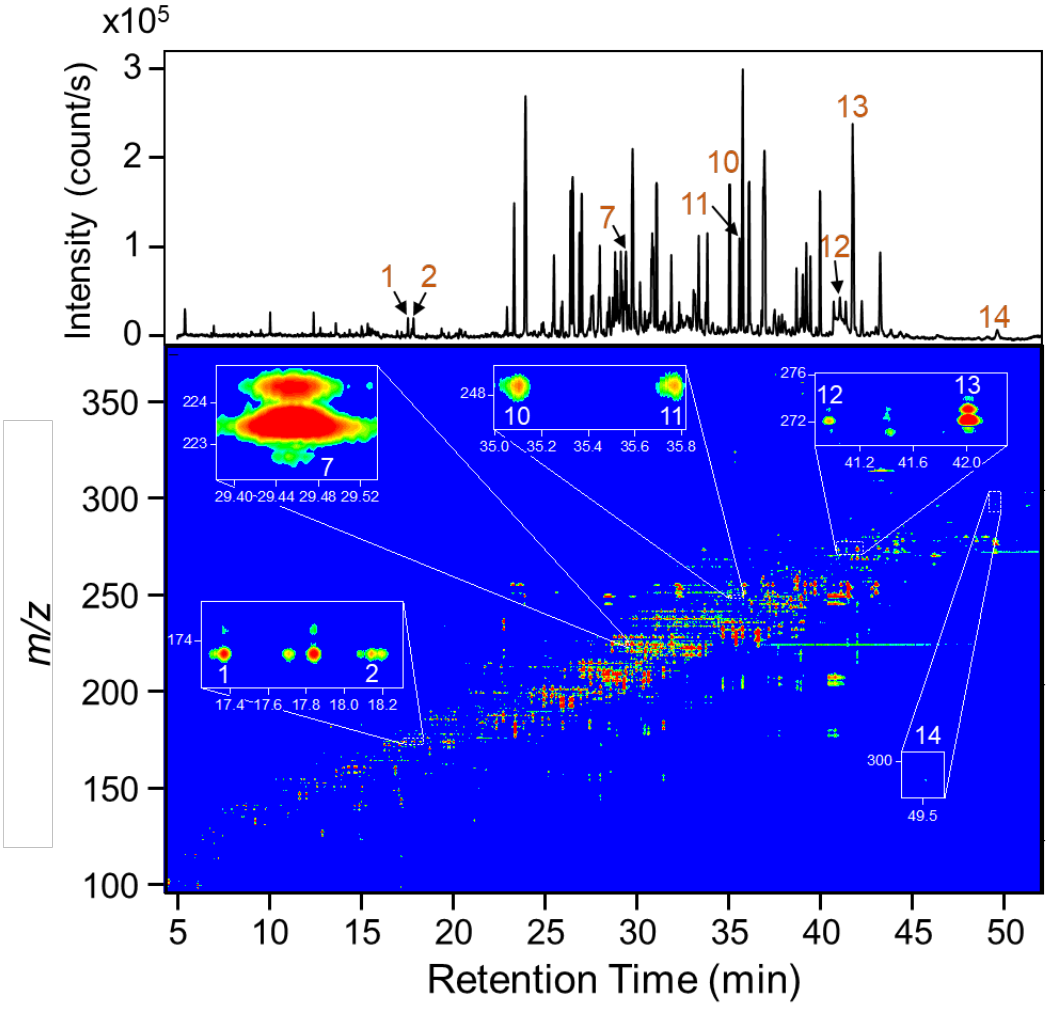

Fig. 5. Two-dimensional display of GC-MS measured for a real sample (SRM1975) ionized at 257 + 343 nm. The delay time was adjusted to t_{DL} = 0. A total ion chromatogram is shown at the top of the figure. The areas of the signals arising from the molecular ions are expanded and are shown in the enclosed squares of the figure. The signal peaks assigned to nitro-PAHs are numbered in the figure (see the chemical structures shown in Fig. 1).

S2). All eight compounds shown in the SRM1975 NIST datasheet were identified in this study. However, the concentrations of nitro-PAHs determined were not necessarily in good agreement with the NIST data. It should be noted that the signal arising from a molecular ion was clearly observed and the purity of the signal peak can be evaluated from the distribution of the intensity of the isotopomer peaks in this study (e.g., see the signals observed for 4-nitroanthracene in Fig. 5). Accordingly, the effect of interferences in the sample matrix were minimal in this study. However, the sample was prepared a long time ago (before 1997) and nitro-PAHs could have partly decomposed or reacted during this period of sample storage.

4. Conclusion

In this study, 14 nitro-PAHs were measured by fsLIMS using a femtosecond Yb laser as the ionization source, based on single-color ionization at 343, 257, 206 nm and two-color ionization at 257 and 343 nm. This analytical system was more useful than EIMS in terms of observing a molecular ion, since the excess energy remaining in the ionic state can be reduced by optimizing the laser wavelength. This advantage was successfully used for a more reliable identification of analytes in a complex sample mixture. A pump-and-probe technique was examined in an attempt to obtain information concerning the lifetime of the excited state, thus providing a useful means for characterization of the analyte. The present technique was several times more sensitive than a large fsLIMS using a complicated Ti:sapphire laser system. Thus, a compact fsLIMS system such as that employed here would have the potential for use in the practical trace analysis of nitro-PAHs in environmental samples.

Credit author statement

Lu Wen: Performed the experimental work and prepared the original draft. Katsunori Yoshinaga: Supervised and assisted in the experimental work. Totaro Imasaka: Supervision of the research and revision of the draft. Tomoko Imasaka: Funding acquisition, supervision, and computational calculations.

Declaration of competing interest

The authors declare that they have no known competing financial interests or personal relationships that could have appeared to influence the work reported in this paper.

Acknowledgements

This research was supported by a Grant-in-Aid for Scientific Research from the Japan Society for the Promotion of Science [JSPS KAKENHI Grant Numbers 20H02399] and by the AMADA Foundation and the Murata Science Foundation. Quantum chemical calculations were mainly carried out using the computer facilities at the Research Institute for Information Technology, Kyushu University. L. W. wishes to acknowledge a scholarship from JST SPRING, Grant Number JPMJSP2136 for financial support to study at Kyushu University.

Appendix A. Supplementary data

Supplementary data to this article can be found online at https://.....

References

[1] J.N. Pitts, K.A. Van Cauwenberghe, D. Grosjean, J.P. Schmidt, D.R. Fitz, W.L. Belser Jr., G.P. Knudson, P.M. Hynds, Atmospheric reaction of polycyclic aromatic hydrocarbons: Facile formation of mutagenic nitro derivatives, Science 202 (1978) 515-519. https://doi.org/10.1126/science.705341.

[2] I.T. Salmeen, A.M. Pero, R. Zator, D. Schuetzle, T.L. Riley, Ames assay chromatograms and the identification of mutagens in diesel particle extracts, Environ. Sci. Techno. 18 (1984) 375-382. https://doi.org/10.1021/es00123a017.

[3] L. He, Y. Lin, D. Day, Y. Teng, X. Wang, X.L. Liu, E. Yan, J. Gong, J. Qin, X. Wang, J. Xiang, J. Mo, Y. Zhang, J.J. Zhang, Nitrated polycyclic aromatic hydrocarbons and arachidonic acid metabolisms relevant to cardiovascular pathophysiology: Findings from a panel study in healthy adults, Environ. Sci. & Technol. 55 (2021) 3867-3875. https://doi.org/10.1021/acs.est.0c08150.

[4] K. Wheelock, J.J. Zhang, R. McConnell, D. Tang, H.E. Volk, Y. Wang, J.B. Herbstman, S. Wang, D.H. Phillips, D. Camann, J. Gong, F. Perera, A novel method for source-specific hemoglobin adducts of nitro-polycyclic aromatic hydrocarbons, Environ. Sci.: Processes & Impacts 20 (2018) 780-789. https://doi.org/10.1016/j.egypro.2017.03.240.

[5] T. Ramdahl, B. Zielinska, J. Arey, R. Atkinson, A.M. Winer, J.N. Pitts Jr., Ubiquitous occurrence of 2-nitrofluoranthene and 2-nitropyrene in air, Nature 321 (1986) 425-427. https://doi.org/10.1038/321425a0.

[6] A. Feilberg, M.W.B. Poulsen, T. Nielsen, H. Skov, Occurrence and sources of particulate nitro-polycyclic aromatic hydrocarbons in ambient air in Denmark,

Atmos. Environ. 35 (2001) 353-366. https://doi.org/10.1016/S1352-2310(00)00142-4.

[7] J.L. Durant, W.F. Busby, A.L. Lafleur, B.W. Penman, C.L. Crespi, Human cell mutagenicity of oxygenated, nitrated and unsubstituted polycyclic aromatic hydrocarbons associated with urban aerosols, Mutat. Res. Genet. Toxicol. 371 (1996) 123-157. https://doi.org/10.1016/S0165-1218(96)90103-2.

[8] B. Zielinska, S. Samy, Analysis of nitrated polycyclic aromatic hydrocarbons, Anal. Bioanal. Chem. 386 (2006) 883-890. https://doi.org/10.1007/s00216-006-0521-3.

[9] W.A. MacCrehan, W.E. May, S.D. Yang, B.A. Benner Jr., Determination of nitro polynuclear aromatic hydrocarbons in air and diesel particulate matter using liquid chromatography with electrochemical and fluorescence detection, Anal. Chem. 60 (1988) 194-199. https://doi.org/10.1021/ac00154a001.

[10] K. Hayakawa, T. Murahashi, M. Butoh, M. Miyazaki, Determination of 1,3-, 1,6-, and 1,8-dinitrophyrenes and 1-nitropyrene in urban air by high-performance liquid chromatography using chemiluminescence detection, Environ. Sci. Technol. 29 (1995) 928-932. https://doi.org/10.1021/es00004a012.

[11] C. Schauer, R. Niessner, U. Pöschl, Analysis of nitrated polycyclic aromatic hydrocarbons by liquid chromatography with fluorescence and mass spectrometry detection: Air particulate matter, soot, and reaction product studies, Anal. Bioanal. Chem. 378 (2004) 725-736. https://doi.org/10.1007/s00216-003-2449-1.

[12] J. Cvačka, J. Barek, A.G. Fogg, J.C. Moreira, J. Zima, High-performance liquid chromatography of nitrated polycyclic aromatic hydrocarbons, Analyst 123 (1998) 9R-18R. https://doi.org/10.1039/A705097F.

[13] T. Paschke, S.B. Hawthorne, D.J. Miller, B. Wenclawiak, Supercritical fluid extraction of nitrated polycyclic aromatic hydrocarbons and polycyclic aromatic hydrocarbons from diesel exhaust particulate matter, J. Chromatogr. A 609 (1992) 333-340. https://doi.org/10.1016/0021-9673(92)80177-V.

[14] M.C. Paputa-Peck, R.S. Marano, D. Schuetzle, T.L. Riley, C.V. Hampton, T.J. Prater, L.M. Skewes, T.E. Jensen, P.H. Ruehle, L.C. Bosch, W.P. Duncan, Determination of nitrated polynuclear aromatic hydrocarbons in particulate extracts by capillary column gas chromatography with nitrogen selective detection, Anal. Cham. 55 (1983) 1946-1954. https://doi.org/10.1021/ac00262a027.

[15] X. Jinhui, F.S.C. Lee, Quantification of nitrated polynuclear aromatic hydrocarbons in atmospheric particulate matter, Anal. Chim. Acta 416 (2000) 111-115. https://doi.org/10.1016/S0003-2670(00)00745-5.

[16] D.L. LaCourse, T.E. Jensen, Determination of 1-nitropyrene in extracts of vehicle particulate emissions, Anal. Chem. 58 (1986) 1894-1895. https://doi.org/10.1021/ac00121a065.

[17] D. Schuetzle, T.L. Riley, T.J. Prater, T.M. Harvey, D.F. Hunt, Analysis of nitrated polycyclic aromatic hydrocarbons in diesel particulates, Anal. Cham. 54 (1982) 265-271. https://doi.org/10.1021/ac00239a028.

[18] R.M. Kamens, F. Zhi-Hua, Y. Yao, D. Chen, S. Chen, M. Vartiainen, A methodology for modeling the formation and decay of nitro-PAH in the atmosphere, Chemosphere 28 (1994) 1623-1632. https://doi.org/10.1016/0045-6535(94)90421-9.

[19] K. Oukebdane, F. Portet-Koltalo, N. Machour, F. Dionnet, P.L. Desbène, Comparison of hot Soxhlet and accelerated solvent extractions with microwave and supercritical fluid extractions for the determination of polycyclic aromatic

hydrocarbons and nitrated derivatives strongly adsorbed on soot collected inside a diesel particulate filter, Talanta 82 (2010) 227-236. https://doi.org/10.1016/j.talanta.2010.04.027.

[20] A.G. Santos, A.C.D. Regis, G.O. da Rocha, M.D.A. Bezerra, R.M. de Jesus, J.B. de Andrade, A simple, comprehensive, and miniaturized solvent extraction method for determination of particulate-phase polycyclic aromatic compounds in the air, J. Chromatogr. A 1435 (2016) 6-17. https://doi.org/10.1016/j.chroma.2016.01.018.

[21] A. Fushimi, S. Hashimoto, T. Ieda, N. Ochiai, Y. Takazawa, Y. Fujitani, K. Tanabe, Thermal desorption-comprehensive two-dimensional gas chromatography coupled with tandem mass spectrometry for determination of trace polycyclic aromatic hydrocarbons and their derivatives, J. Chromatogr. A 1252 (2012) 164-170. https://doi.org/10.1016/j.chroma.2012.06.068.

[22] B. Dušek, J. Hajšlová, V. Kocourek, Determination of nitrated polycyclic aromatic hydrocarbons and their precursors in biotic matrices, J. Chromatogr. A 982 (2002) 127-143. https://doi.org/10.1016/s0021-9673(02)01340-7.

[23] D.Z. Bezabeh, H.A. Bamford, M.M. Schantz, S.A. Wise, Determination of nitrated polycyclic aromatic hydrocarbons in diesel particulate-related standard reference materials by using gas chromatography/mass spectrometry with negative ion chemical ionization, Anal. Bioanal. Chem. 375 (2003) 381-388. https://doi.org/10.1007/s00216-002-1698-8.

[24] A. Albinet, E. Leoz-Garziandia, H. Budzinski, E. Villenave, Simultaneous analysis of oxygenated and nitrated polycyclic aromatic hydrocarbons on standard reference material 1649a (urban dust) and on natural ambient air samples by gas

chromatography-mass spectrometry with negative ion chemical ionization, J. Chromatogr. A 1121 (2006) 106-113. https://doi.org/10.1016/j.chroma.2006.04.043.

[25] B.S. Crimmins, J.E. Baker, Improved GC/MS methods for measuring hourly PAH and nitro-PAH concentrations in urban particulate matter, Atoms. Environ. 40 (2006) 6764-6779. https://doi.org/10.1016/j.atmosenv.2006.05.078.

[26] H.A. Bamford, D.Z. Bezabeh, M.M. Schantz, S.A. Wise, J.E. Baker, Determination and comparison of nitrated-polycyclic aromatic hydrocarbons measured in air and diesel particulate reference materials, Chemosphere 50 (2003) 575-587. https://doi.org/10.1016/S0045-6535(02)00667-7.

[27] R. Zimmermann, W. Welthagen, T. Gröger, Photo-ionisation mass spectrometry as detection method for gas chromatography: Optical selectivity and multidimensional comprehensive separations, J. Chromatogr. A 1184 (2008) 296-308. https://doi.org/10.1016/j.chroma.2007.08.081.

[28] N. Tsuji, Y. Matsuzaki, S. Hayashi, Real-time detection of 1-nitronaphthalene in atmosphere by single-photon ionization mass spectrometry, Bunseki Kagaku 61 (2012) 359-365. https://doi.org/10.2116/bunsekikagaku.61.359.

[29] R.N. Dotter, C.H. Smith, M.K. Young, P.B. Kelly, A. Daniel Jones, E.M. McCauley, D.P.Y. Chang, Laser desorption/ionization time-of-flight mass spectrometry of nitrated polycyclic aromatic hydrocarbons, Anal. Chem. 68 (1996) 2319-2324. https://doi.org/10.1021/ac951132r.

[30] D.Z. Bezabeh, T.M. Allen, E.M. McCauley, P.B. Kelly, A.D. Jones, Negative ion laser desorption ionization time-of-flight mass spectrometry of nitrated polycyclic aromatic hydrocarbons, J. Am. Soc. Mass Spectrom. 8 (1997) 630-636. https://doi.org/10.1016/S1044-0305(97)00078-0.

[31] A.D. Tasker, L. Robson, K.W.D. Ledingham, T. McCanny, P. McKenna, C. Kosmidis, D.A. Jaroszynski, Femtosecond ionization and dissociation of laser desorbed nitro-PAHs, Int. J. Mass Spectrom. 225 (2003) 53-70. https://doi.org/10.1016/s1387-3806(02)01045-x.

[32] T. Imasaka, T. Imasaka, Femtosecond ionization mass spectrometry for chromatographic detection, J. Chromatogr. A 1642 (2021) 462023. https://doi.org/10.1016/j.chroma.2021.462023.

[33] Y. Tang, T. Imasaka, S. Yamamoto, T. Imasaka, Multiphoton ionization mass spectrometry of nitrated polycyclic aromatic hydrocarbons, Talanta 140 (2015) 109-114. https://doi.org/10.1016/j.talanta.2015.03.027.

[34] Y. Tang, T. Imasaka, S. Yamamoto, T. Imasaka, Determination of polycyclic aromatic hydrocarbons and their nitro-, amino-derivatives adsorbed on particulate matter 2.5 by multiphoton ionization mass spectrometry using far-, deep-, and near-ultraviolet femtosecond lasers, Chemosphere 152 (2016) 252-258. https://doi.org/10.1016/j.chemosphere.2016.02.114.

[35] N. Itouyama, T. Matsui, S. Yamamoto, T. Imasaka, T. Imasaka, Analysis of parent/nitrated polycyclic aromatic hydrocarbons in particulate matter 2.5 based on femtosecond ionization mass spectrometry, J. Am. Soc. Mass Spectrom. 27 (2016) 293-300. https://doi.org/10.1007/s13361-015-1276-x.

[36] A. Li, T. Imasaka, T. Imasaka, Optimal laser wavelength for femtosecond ionization of polycyclic aromatic hydrocarbons and their nitrated compounds in mass spectrometry, Anal. Chem. 90 (2018) 2963−2969. https://doi.org/10.1021/acs.analchem.8b00125.

[37] T. Fujii, T. Imasaka, T. Imasaka, Use of chemical conversion for determination of nitrated aromatic hydrocarbons using femtosecond ionization mass spectrometry, Anal. Chim. Acta 996 (2017) 48-53. https://doi.org/10.1016/j.aca.2017.09.049.

[38] Y. Tang, S. Yamamoto, T. Imasaka, Determination of nitrated polycyclic aromatic hydrocarbons in particulate matter 2.5 by laser ionization mass spectrometry using an on-line chemical-reduction system, Analyst 144 (2019) 2909-2913. https://doi.org/10.1039/C9AN00308H.

[39] K. Yoshinaga, N.V. Hao, T. Imasaka, T. Imasaka, Miniature time-of-flight mass analyzer for use in combination with a compact highly-repetitive femtosecond laser ionization source, Anal. Chim. Acta 1203 (2022) 339673. https://doi.org/10.1016/j.aca.2022.339673.

[40] C. Kosmidis, K.W.D. Ledingham, H.S. Kilic, T. McCanny, R.P. Singhal, A.J. Langley, W. Shaikh, On the fragmentation of nitrobenzene and nitrotoluenes induced by a femtosecond laser at 375 nm, J. Phys. Chem. A 101 (1997) 2264-2270. https://doi.org/10.1021/jp963187i.

[41] V. Schäfer, K-M. Weitzel, Qualitative and quantitative distinction of ortho-, meta-, and para-fluorotoluene by means of chirped femtosecond laser ionization, Anal. Chem. 92 (2020) 5492-5499. https://doi.org/10.1021/acs.analchem.0c00234.

[42] J. A. Noble, C. Aupetit, D. Descamps, S. Petit, A. Simon, J. Mascetti, N. B. Amor, V. Blanchet, Ultrafast electronic relaxations from the S_3 state of pyrene, Phys. Chem. Chem. Phys. 21 (2019) 14111-14125. DOI: 10.1039/c8cp06895j.

[43] T. Imasaka, T. Okuno, T. Imasaka, The search for a molecule to measure an autocorrelation trace of the second/third harmonic emission of a Ti:sapphire laser based on two-photon resonant excitation and subsequent one photon ionization, Appl.

Phys. B, Lasers and Optics 113 (2013) 543-549. https://doi.org/10.1007/s00340-013-5505-3.

[44] R. Morales-Cueto, M. Esquivelzeta-Rabell, J. Saucedo-Zugazagoitia, J. Peon, Single excited-state dynamics of nitropolycyclic aromatic hydrocarbons: Direct measurements by femtosecond fluorescence up-conversion, J. Phys. Chem. A 111 (2007) 552-557. https://doi.org/10.1021/jp065364d.

[45] S. Murudkar, A.K. Mora, P.K. Singh, S. Nath, Origin of ultrafast excited state dynamics of 1-nitropyrene, J. Phys. Chem. A 115 (2011) 10762-10766. https://doi.org/10.1021/jp205946c.